



Immune checkpoint CD155 promoter methylation profiling reveals cancer-associated behaviors within breast neoplasia

Hana Triki¹ · Ken Declerck² · Slim Charfi³ · Wala Ben Kridis⁴ · Kais Chaabane⁵ · Sawssan Ben Halima⁵ · Tahya Sellami³ · Ahmed Rebai¹ · Wim Vanden Berghe² · Boutheina Cherif¹

Received: 7 August 2021 / Accepted: 23 September 2021 / Published online: 4 October 2021
© The Author(s), under exclusive licence to Springer-Verlag GmbH Germany, part of Springer Nature 2021

Abstract

BACKGROUND CD155 immune checkpoint has recently emerged as a compelling immunotherapeutic target. Epigenetic DNA methylation changes are recognized as key molecular mechanisms in cancer development. Hence, the identification of methylation markers that are sensitive and specific for breast cancer may improve early detection and predict prognosis. We speculate that CD155 promoter methylation can be a valuable epigenetic biomarker, based upon strong indications for its immunoregulatory functions.

METHODS Methylation analyses were conducted on 14 CpGs sites in the CD155 promoter region by bisulfite pyrosequencing. To elucidate the related gene expression changes, a transcriptional study using RT-qPCR was performed. Statistical analyses were performed to evaluate correlations of CD155 methylation profiles with mRNA expression together with clinical-pathological features, prognosis and immune infiltrate.

RESULTS CD155 promoter methylation profile was significantly associated with SBR grade, tumor size, molecular subgroups, HER2 and hormonal receptors expression status. Low CD155 methylation rates correlated with better prognosis in univariate cox proportional hazard analysis and appeared as an independent survival predictor in cox-regression multivariate analysis. Further, methylation changes at CD155 specific CpG sites were consistent with CD155 membranous mRNA isoform expression status. Statistical analyses also showed a significant association with immune Natural Killer cell infiltrate when looking at the CpG7, CpG8, CpG9 and CpG11 sites.

CONCLUSION Altogether, our results contribute to a better understanding of the impact of CD155 immune checkpoint modality expression in breast tumors, revealing for the first time that specific CpG sites from CD155 promoter may be a potential biomarker in breast cancer monitoring.

Keywords CD155 · Immune checkpoint · DNA methylation · mRNA expression · Breast cancer

✉ Boutheina Cherif
boutheina.cherif@isbs.usf.tn;
boutheina.cherif.cbs@gmail.com

¹ Laboratory of Molecular and Cellular Screening Processes, Centre de Biotechnologie de Sfax, University of Sfax, B.P 1177, 3018 Sfax, Tunisia

² Laboratory of Protein Chemistry, Proteomics and Epigenetic Signaling (PPES) and Integrated Personalized and Precision Oncology Network (IPPON), Department of Biomedical Sciences, University of Antwerp, Antwerp, Belgium

³ Department of Pathology, University Hospital Habib Bourguiba, Sfax, Tunisia

⁴ Department of Medical Oncology, University Hospital Habib Bourguiba, Sfax, Tunisia

⁵ Department of Gynecology, University Hospital Hédi Chaker, Sfax, Tunisia

Abbreviations

ACTB	Beta-Actin
bp	Base pair
<i>cyt</i> -CD155	Cytoplasmic CD155
DFS	Disease-Free Survival
FFPE	Formalin-Fixed and Paraffin-Embedded
HER2	HER2 positive
kbp	Kilobase pair
LA	Luminal A
LB-Like	Luminal B like
<i>m</i> -CD155	Membranous CD155
NK	Natural Killer
NK-TILs	Tumor-Infiltrating Natural Killer Cell
OS	Overall Survival
RT-qPCR	Real-time Quantitative Reverse Transcriptase Polymerase Chain Reaction

SBR	Scarff-Bloom-Richardson
TBE	Tris-Borate-EDTA
TILs	Tumor-Infiltrating Lymphocytes
TME	Tumor Microenvironment
TNBC	Triple Negative breast cancer
TNM	Tumor lymph node and metastases

Introduction

Immune checkpoint molecules act in co-stimulatory and inhibitory pathways that tightly regulate the immune response and maintain self-tolerance under normal physiological conditions. Tumors have been shown to dysregulate these pathways to build immune resistance mechanism creating an immunosuppressive microenvironment leading to immune evasion of cancerous cell [1, 2]. Indeed, extensive studies revealed a crucial role for the immune system both in tumor suppression and promotion, by regulating adaptive and innate immune pathways involving especially T cells and Natural killer (NK) cells. Therefore, immune checkpoints molecules which target these immunoregulatory pathways hold promise to strengthen the body's immunological function against tumors [3].

The most known immune checkpoint regulators are programmed cell death 1 (PD-1)/PD-1 ligand 1 (PD-L1), cytotoxic T lymphocyte antigen-4 (CTLA-4), T cell immune receptor with immunoglobulin (Ig) and ITIM domains (TIGIT) [4, 5], and several others are currently being evaluated as potential therapeutic targets to improve the anti-tumor immunity. Recently, TIGIT and its ligand poliovirus receptor (PVR, CD155) have entered the limelight as novel immune checkpoints [6]. Besides, CD155 has an immunoregulatory potential upon interaction with the co-stimulatory immune receptor CD226 (DNAM-1) and the inhibitory checkpoint receptors TIGIT and CD96, which are differentially regulated at the cell surface of NK cells and T cells [6, 7]. The integration of signals from CD155 cognate receptors results in activation or inhibition of NK cell-mediated innate immunity. In addition, CD155 overexpression has also been observed in various tumor types, including colon cancer, lung adenocarcinoma, melanoma, pancreatic cancer glioblastoma [8–12] and breast cancer [13–15]. Interestingly, we have recently reported the clinical significance and the prognostic value of CD155 protein expression in human breast cancer [14]. CD155 can be expressed in the cytoplasm or at the plasma membrane level, suggesting different immunoregulatory roles in the tumor microenvironment. Moreover, CD155 undergoes alternative splicing, generating four unique splice isoforms [16, 17]. It can be produced as soluble forms lacking the transmembrane domain, encoded by alternative splicing isoforms β and γ [18], or as a membrane-bound protein encoded by two alternative splicing forms,

α and δ , referenced as the transmembrane isoforms [17]. Whereas transmembrane CD155 acts as an activating ligand of NK cells and cytotoxic T lymphocytes (CTLs), other studies suggest that overexpression of soluble CD155 isoforms could act as a cancer-specific immune resistance mechanism against the cell-mediated immune response by masking the signaling effect of transmembrane CD155 isoform [19].

Moreover, expression of immune checkpoint molecules is further controlled by epigenetic mechanisms which add another regulatory layer to immune modulation. Since aberrant hypermethylation/hypomethylation patterns frequently result in adverse tumorigenic gene expression and impaired immune checkpoint regulation, differentially methylated loci might represent useful biomarkers in immune-oncology [20, 21]. More precisely, studies showed that altered gene expression and/or deregulated epigenetic machineries display central roles in the onset and progression of breast cancer [22]. Particularly, DNA promoter methylation studies in patients with breast cancer using normal and cancer tissues showed hypomethylation irrespective of the immune checkpoint PD-L1 expression status [23]. Accordingly, a number of clinical biomarker assays are needed for early detection and to predict prognosis of cancer, combining therapies of DNA demethylating agents with immune checkpoint inhibitors [24, 25].

Therefore, we studied the differential expression of immune checkpoint CD155 in relation to its promoter methylation pattern in breast cancer patients.

Material and methods

Study population and tumor samples

This is a retrospective cohort study of females diagnosed with invasive breast carcinoma who underwent surgical resection prior to any treatment at the Department of Gynecology and Obstetrics of the Hedi Chaker University Hospital in the south of Tunisia. All procedures performed in this study were in compliance with the ethical standards of the institutional and the national research committee of Habib Bourguiba University Hospital and with the 1964 Helsinki declaration and its later amendments or comparable ethical standards. We collected a total of $n = 116$ well characterized primary breast cancer tissues, and $n = 11$ non-tumor breast tissue samples from women without cancer used as healthy control. Samples were retrieved from the tumor bank of the Department of Pathology of the Habib Bourguiba University Hospital (Sfax, Tunisia), and they included 101 frozen tissues and 15 formalin-fixed and paraffin-embedded (FFPE) tissues. The clinical-pathological data acquired by retrospective medical records included age, histological grade, histological type, molecular subtype, tumor size, lymph

node status, distant metastasis, lymphovascular invasion, menopausal status, adjuvant therapy status and clinical stage according to the 8th edition of TNM (tumor, node, metastasis) classification adopted by the International Union Against Cancer. The clinical-pathological characteristics of 116 breast cancer patients are summarized in Supplementary Table 1. Overall survival (OS) and disease-free survival (DFS) were investigated to evaluate CD155 influence upon patient prognosis at the department of medical oncology of the Habib Bourguiba University Hospital (Sfax, Tunisia). The overall follow-up time ranged from 1 to 151 months, with a median follow-up of 78.5 months, during which 25 patients underwent cancer relapse and 29 died.

Breast cancer subtyping

Breast cancer molecular classification is based on the expression of classical biomarkers including estrogen (ER) and progesterone (PR) receptor, the human epidermal growth factor receptor 2 (HER2) and Ki-67 labeling index as a cell proliferation biomarker. Expression of all biomarkers was carried out using immunohistochemical method. Hormone receptors (ER and PR) were considered positive when > 1% of infiltrating tumor cell nuclei were stained. Tumors were considered positive for HER2 if immunostaining was scored as 3+ according to Wolff criteria [26] and cancers with HER2 scored as 2+ (indeterminate) were assessed through fluorescent in situ hybridization [FISH]. Ki-67 was visually scored for percentage of tumor cell nuclei with positive immunostaining above the background level using a cutoff at 20% of expression. Five molecular subtypes were defined: Luminal A (LA) if ER/PR+, HER2- and Ki-67 < 20%; Luminal B like (LB-Like) if ER/PR+, HER2- and Ki-67 > 20%; Luminal B (LB) if ER/PR+ and HER2+; HER2 positive (HER2) if ER/PR- and HER2+; Triple Negative Breast Cancer (TNBC) if ER/PR- and HER2- as described previously [14].

Immune infiltrate evaluation

TILs evaluation was performed by a standardized methodology which relies on visual assessment of hematoxylin and eosin sections. According to the international TILs Working group recommendations, TILs were detected by a semiquantitative evaluation by light microscopy. Briefly, all inflammatory mononuclear cells in the stromal compartment within the borders of the invasive tumor were evaluated and reported as a percentage than as a level (TILs grade). TILs outside the tumor border, around ductal carcinoma in situ and normal breast tissue, as well as in areas of necrosis, were not taken into account. TILs expression levels were classified into three grades: low (0–10%), medium (10%–50%), and high (50%–90%) as described previously [27]. NK-TILs

infiltration was assessed by immunohistochemistry using the anti-CD56 antibody (NCL-L CD56-1B6, Leica Novocastrol). NK-TILs were evaluated as CD56+ lymphocytes tissues count and distribution in ten randomly selected areas and then evaluated at higher magnification (×40 objectives). Scoring of NK-TILs immunostaining was determined as low (negative or weak) cell presence or high (moderate or strong) cell presence by a cutoff value of five cells as described previously [14].

DNA extraction and qualification

Five 10-μm-thick OCT (OptimalCutting Temperature compound)-embedded frozen tissue and FFPE tissue sections were cut for each case. Sample matched genomic DNA was extracted by standard Proteinase K digestion with slight modification [28], followed by phenol–chloroform extraction and ethanol precipitation. FFPE tissues were deparaffinized in xylene followed by subsequent rehydration through graded alcohols prior to any extraction step. For each case, tissues were homogenized in 490 μl of proteinase K buffer (0.5 M EDTA pH 8, 2 M Tris, 1.5 M NaCl, H₂O) with a mixer mill (MM 400, RETSCH) using adapter Rack for 10 Reaction Vials and 10 mm stainless steel grinding balls at 30 Hz for 1 min. Samples were then incubated with 10 μl proteinase K (20 mg/ml) at 56 °C for four hours, after incubation, the tissue dissolves completely. DNA was extracted by adding an equal volume of phenol–chloroform-isoamyl alcohol (25: 24: 1) and precipitated overnight with sodium acetate and ethanol at –20 °C. The DNA pellet of each sample was collected by centrifugation for 20 min at 4 °C purified with cold 70% ethanol and air dried at room temperature. DNA was resuspended in 20 μl of sterile distilled water. Extraction yield was evaluated with Nanodrop2000 spectrophotometer (Thermo Scientific, Wilmington, DE, USA). Extracted DNAs were then assessed for their integrity by a control PCR reaction designed to amplify a fragment of 250 bp of the β-globin gene as described previously [29].

DNA bisulfite conversion and qualification

Genomic DNA (500 ng) was bisulfite converted using the EZ DNA methylation kit (Zymo Research, Cambridge Bioscience, Cambridge, UK) according to manufacturer's instructions. Bisulfite-treated genomic DNA was re-quantified using a Qubit 4.0 fluorometer (Life Technologies) according to the manufacturer's protocol. Successful bisulfite conversion was confirmed by the amplification of a 208 bp amplicon of the *SALL3* gene as described previously [30], under the following conditions: 95 °C 15 min; then 45 cycles of 94 °C 30 s, 55 °C for 30 s, 72 °C for 30 s; followed by 72 °C for 10 min using the primer set: *SALL3*-Fw:5'-GTTTGGGTTTGTTTGGTTT-3'; *SALL3*-Rev:5'-ACCCTTACCAATCT

CTTAACTTTC-3'. Successful PCR amplification was evaluated by TBE (Tris-Borate-EDTA) electrophoresis at 2% agarose gel and visualized by GelRed™ staining.

CD155 pyrosequencing

For CpG site-targeted bisulfite pyrosequencing, we used the PyroMark assay design 2.0 software for forward, biotinylated-reverse and sequencing CD155 primers design. Targets of interest were PCR amplified using the PyroMark PCR kit (Qiagen, Hilden, Germany) according to manufacturer's instructions. For each sample, 50 ng of bisulfite-treated DNA was subsequently used for PCR amplification in a final volume of 25 µL containing 10 µM of forward primer and biotin-labeled reverse primer. The primers sequences are summarized in Table 1. Cycling conditions started with an initial PCR activation at 95 °C for 15 min, then 45 cycles of 95 °C for 30 s, 56 °C for 30 s, 72 °C for 30 s, followed by a final extension at 72 °C for 10 min. Successful PCR amplification was confirmed by TBE electrophoresis at 2% agarose gel and visualized by GelRed™ staining.

After the amplification, pyrosequencing was performed using the PyroMark Advanced Q24 System according to the manufacturer's guidelines (Qiagen, Hilden, Germany). In brief, Biotin-labeled PCR products were immobilized on Streptavidin-coated Sepharose beads (High Performance, GE Healthcare, Uppsala, Sweden) in the PyroMark binding buffer (Qiagen, Hilden, Germany). The mixtures were agitated at room temperature for 15 min under constant mixing (1400 rpm). The DNA-coated beads were subsequently captured by the PyroMark vacuum Q24 workstation, washed and denatured. The beads with single-stranded DNA templates were then released into a 24-well plate with 20 µl of PyroMark annealing buffer (Qiagen, Hilden, Germany) containing the corresponding sequencing primer at a final concentration of 0.4 µM (Table 1) for 2 min at 80 °C. The PyroMark plate was placed into a PyroMark Q24 Advanced instrument (Qiagen, Hilden, Germany), and the sequencing procedure was performed by the cyclic dispensation of substrates, enzymes, and four different nucleotides in a pre-specified order (PyroMark Advanced Reagents, Qiagen, Hilden, Germany). Following pyrosequencing, the completed run files were imported into PyroMark Q24 Advanced

software (version 3.0.0; Qiagen) and cytosine methylation was quantified.

RNA extraction and real-time reverse transcriptase polymerase chain reaction analysis

Frozen tissues (30 mg) were disrupted using a mixer mill (MM 400, RETSCH) until they are uniformly homogeneous. Total RNA was isolated from frozen tissues using the AllPrep DNA/RNA Mini Kit (Qiagen) according to the manufacturer's protocol. Extraction yield was evaluated with Nanodrop2000 spectrophotometer (Thermo Scientific, Wilmington, DE, USA). First-strand cDNA was synthesized from 1 µg of total RNA using PrimeScript RT reagent Kit (Takara Bio Inc., Otsu, Japan) according to the manufacturer's recommendations. cDNAs were used as template for PCR using specific primers for CD155 and β-Actin (housekeeping gene/endogenous control). All samples were done in duplicate for both target and reference gene. Real-time quantitative PCR (RT-qPCR) was performed in a CFX96 Real-Time PCR detection system (Bio-Rad, Hercules, CA, USA) and carried out in a final volume of 10 µl using 5ng of cDNA, 0.3 µl of each primer (10 µM), 5 µl of the TB Green Premix Ex Taq II (TliR-NaseH Plus, Takara Bio, Japan) and RNase free water (DEPC-Treated). The thermal cycling conditions were as follows: 30 s at 95 °C and 39 cycles of 10 s at 95 °C, 30 s at 64 °C and 5 s at 72 °C.

CD155 primer set was carefully designed to amplify relevant transcripts without genomic DNA contamination. PCR primer sequences were as follows: *CD155*-Fw: 5'-ACTCAGGCATGTCCCGTAAC-3' and *CD155*-Rev: 5'-CTGTACTCGAGGGACACAGATG-3'; for β-Actin amplification the following primer set was used: *β-Actin*-Fw: 5'-CATCGAGCACGGCATCGTCA-3' and *β-Actin*-Rev: 5'-TAGCACAGCCTGGATAGCAAC-3' (211 bp). Melt curve analysis was performed for all PCR products following RT-PCR run using the Bio-Rad CFX Manager software 3.1 (Bio-Rad, Redmond, WA, USA). The CD155 mRNA expression level is given as relative copy numbers normalized against β-Actin housekeeping gene transcripts.

Table 1 Sequences and amplicon size of primers used for CD155pyrosequencing

Gene	PCR primers	Product length	Sequencing primer
CD155	5'-ATTTGGAATGTG GGAGATTTTATA TAGGAA-3' 5'-BIOTIN-AAACCA CCCAAACCTAAC C-3'	142 bp	5'-GAAGTAGTTTTTTTTAGTGGGTA-3'

Statistical analysis

The methylation data imported into R studio (version 3.6.1) were processed, correlations of the methylation percentages results with patients clinical-pathological features and with CD155 expression levels were assessed with Student's *t* test and Anova test.

In multivariate analysis, the calculation of the hazard ratios and their 95% confidence interval was carried out using a Cox model. Survival analyses were performed using SPSS 20.0 statistical software for Windows (SPSS Inc., IBM).

For all the statistical tests used in this work, associations were retained as significant for a *p* value ≤ 0.05 .

Results

Genomic designing and technical concept for CD155 promoter methylation analysis

Primer sets with one biotin-labeled primer were used to amplify the bisulfite converted DNA. New primers for CD155 gene were designed using PyroMark Assay Design software version 2.0 (Qiagen), amplicons were kept short with lengths between 90 and 150 base pairs (bp) to enable subsequent studies on FFPE specimens. Primers were

located in promoter CpG islands identified by MethPrimer, depending on where the design of the assay allowed for optimal primers. Due care was taken to avoid any primer overlapping CG dyads to prevent amplification biases.

The choice of the genomic region sensitive to methylation was carried out by the CpGs island prediction software the Li Lab Tools and Databases (<http://www.urogene.org/cgi>). CD155 genomic sequence was extracted from genomic databases (Genome Browser) by adopting the annotation proposed by Ensembl genome browser (<http://www.ensembl.org>). Selection was performed on the entire genomic sequence with the addition of 2 kbp in upstream of its first ATG.

Li Lab Tools Software displays the potential CpGs island of the submitted selection, regions with the highest score were considered for primers design. The in-silico study showed that the CD155 gene has eight exons and seven introns and that the first 2000 nucleotides of its promoter contain a single CpG island (Fig. 1).

Regions of interest were then submitted to the software provided by Qiagen "PyroMark Assay Design 2.0." The corresponding converted sequence after bisulfite treatment was provided, and the corresponding primer sets are automatically generated containing both PCR primers and sequencing primers. Each set of primers is associated with a quality index assigned in the form of a score based on several parameters specific to the pyrosequencing analysis. The

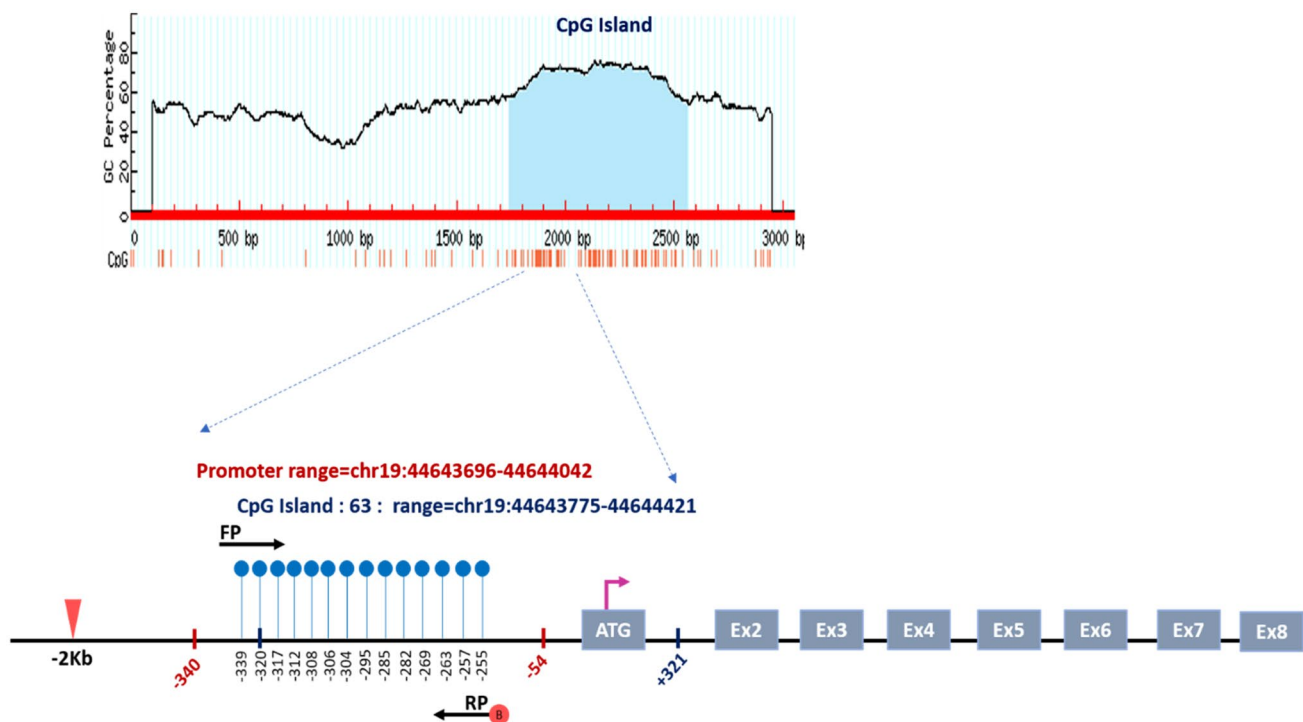


Fig. 1 Schematic representation of the human CD155 gene with its promoter region and selected CpG Island. The studied 14 CpG sites are shown as lollipops within the promoter range

selected primer set had a score equal to 80%. The reverse primer of the selected primer set has the particularity of being coupled to a biotin molecule, allowing its purification during pyrosequencing. We quantified methylation percentages of the CpG sites of CD155 gene promoter by pyrosequencing using a CD155 sequencing primer. The targeted region in our study displays 14 CpG sites (Fig. 1). According to UCSC genome browser and ENCODE data, this region is located in a CpG island encompassing several enhancers and regulatory elements, suggesting that this region is involved in the active transcription of CD155.

Evaluation of CpG sites methylation rates of CD155 gene promoter by pyrosequencing

CD155 promoter methylation was investigated in 116 primary breast carcinoma samples taken from FFPE and frozen cancerous breast tissue biopsies. In addition, 11 healthy breast samples taken from frozen tissues were included in our study as healthy controls. The pyrograms obtained display methylation rates calculated by comparing the heights of C and T peaks at each CpG site. The results of pyrosequencing of the selected region show that the methylation rates are relatively low and range between 1 and 46%. FFPE samples were successfully analyzed and were therefore included for pyrosequencing analysis, samples ranged in their degree of methylation between 0% and 43.02%. Likewise, frozen samples were successfully analyzed and were further investigated for their promoter methylation. Frozen cancerous breast tissue DNAs ranged in their degree of methylation between 0% and 45.83%, while healthy frozen samples ranged between 0% and 30.08%. To ensure our results credibility, samples were pooled for subsequent analyses taking into account the significant difference between FFPE and frozen samples using correction coefficient.

Statistical analyses showed no evidence for significant differences in global methylation level (overall methylation mean percentage) of cancer tissues as compared to healthy controls, although cancer tissues were slightly higher in methylation (p value = 0.508).

Association between CD155 methylation status, clinical indicators and immune infiltrate data

Table 2 summarizes all the correlations established between the CD155 gene promoter CpG sites methylation status and the clinicopathological data. We evaluated the differences in global DNA methylation according to clinical-pathological features. Although methylation appeared to be higher for the tumor SBR grades II and III, the correlation did not reach statistical significance (p value = 0.064, Fig. 2a). However, a significant correlation was found between CD155 methylation status and tumor size where higher levels of methylation

were correlated with higher tumor size (p value = 0.001, Fig. 2b).

Statistical analyses also showed a significant association with molecular groups. Most importantly, the Her2, LB and TNBC groups had almost the same trend with higher global methylation rates compared to the LB-like and LA groups (p value = 0.00343, Fig. 2c). On the other hand, statistical analysis showed a significant and positive correlation between a higher methylation and the expression of the HER2 receptor (p value = 0.005, Fig. 2d). Meanwhile, negative correlations with progesterone (RP) and estrogen (RE) receptors expression status (p value = 0.007 and p value = 0.03, respectively, Fig. 2e, f) were found.

Next, we assessed the difference in overall methylation mean percentage according to tumor-infiltrating lymphocytes (TILs) and NK cells (NK-TILs) in breast cancer patients. No association with the immune infiltrate was found (Table 2).

Profiling of differentially methylated CpG sites related to clinical-pathological data

We determined which of the 14 individual CpG sites were better suited to be related to clinical-pathological indicators, we therefore scanned the entire region to refine our search. Table 3 reports the different correlations between the methylation rates of the 14 individual CpG sites and clinical-pathological features. With SBR grade, a statistically significant difference in methylation between the three groups was observed when looking at CpG7 and CpG9 (p value = 2.17×10^{-2} , p value = 2.46×10^{-2} , respectively) with the same trend observed when comparing global methylation mean percentage with SBR grade. Moreover, a significant correlation was found with molecular group, this difference is observed in almost all CpG sites particularly in CpG1, CpG3 to CpG10, CpG12 and CpG13. Statistical analysis also demonstrated significant associations with the expression of the HER2 receptor, a positive correlation between higher methylation rates and a HER2 + status was observed, the differences were significant for CpG2 to CpG10 and CpG13 sites. On the other hand, a negative correlation with the receptors of RP and RE was found where RE + and RP + tumors were lower in methylation at CpG1, CpG3 to CpG9 and CpG13 sites for the RE receptor, and the CpG4 to CpG9 and CpG13 sites for the RP receptor. In addition, a significant association was found between methylation status of all CpG sites and tumor size where larger tumors were higher in methylation compared to tumors with lower size. Further, we found a significant association with metastasis when looking at CpG4 where a higher methylation percentage correlated positively with metastasis.

Statistical analyses also showed a significant association with NK cell infiltration when looking at the CpG7, CpG8,

Table 2 Associations of CD155 promotor methylation (overall mean methylation or sub_mean methylation values) and CD155 mRNA expression (normalized counts) with clinical-pathological and immunological parameters

Variable	N (%)			Mean Methylation			Sub_mean Methylation			mRNA expression ($2^{\Delta\Delta Ct}$)			
	Mean \pm SD	Min	Max	Mean \pm SD	Min	Max	Mean \pm SD	Min	Max	Mean \pm SD	Min	Max	p value
Age													
≤40	18.1	3.5 ± 4.6	0.19	19.41	0.191	19.41	3.58 ± 6.06	0	24.68	2.47 ± 5.5	0.05	25.29	0.707
>40	81.9	4.01 ± 6.27	0.62	40.56	0.545	40.56	4 ± 6.82	0.51	40.38	2.18 ± 2.92	0.007	15.84	0.858
Menopausal Status													
Menopausal	52.6	4.25 ± 6.9	0.62	40.56	0.064	40.56	4.2 ± 7.5	0.51	40.38	2.2 ± 2.9	0.013	15.84	0.207
Premenopausal	47.4	3.63 ± 4.81	0.19	23.67	0.064	23.67	3.6 ± 5.7	0	24.68	2.3 ± 4.2	0.007	25.29	0.207
SBR													
I	18.1	1.55 ± 0.5	0.54	2.7	0.003	2.7	1.34 ± 0.39	0.51	2.16	1.35 ± 1.27	0.02	4.34	0.787
II	37.9	3.96 ± 5.35	0.19	29.23	0.003	29.23	3.95 ± 6.04	0	27.6	3.05 ± 4.9	0.02	25.29	0.787
III	44	4.91 ± 7.34	0.69	40.56	0.003	40.56	4.94 ± 8.16	0.62	40.38	1.97 ± 2.78	0.007	15.84	0.787
GM													
LA	25.9	1.63 ± 0.67	0.54	3.3	0.631	3.3	1.37 ± 0.43	0.66	2.16	1.95 ± 2.62	0.02	11.39	0.045
LB	12.9	5.75 ± 6.98	1.03	29.23	0.631	29.23	5.67 ± 7	0.83	27.6	2.96 ± 6.87	0.007	25.29	0.045
LB-Like	32.8	2.8 ± 3.44	0.19	19.41	0.228	19.41	2.25 ± 3.15	0	19.19	2.48 ± 3.23	0.03	15.48	0.612
HER2	11.2	7.2 ± 6.89	1.58	19.44	0.228	19.44	8.94 ± 9.92	1.26	26.11	1.01 ± 1.37	0.02	4.3	0.612
TNBC	17.2	6.06 ± 9.59	0.74	40.56	0.228	40.56	6.2 ± 9.87	0.74	40.38	2.22 ± 2.39	0.04	7.16	0.612
Histological type													
CCI	80.2	3.25 ± 5.77	0.19	40.56	0.631	40.56	3.79 ± 6.47	0	40.38	1.86 ± 3.33	0.007	25.29	0.045
Others	19.8	4.44 ± 6.79	0.62	29.23	0.228	29.23	4.39 ± 7.46	0.51	27.6	3.66 ± 4.08	0.04	15.84	0.612
Lymphovascular invasion													
No	59.5	3.44 ± 5.95	0.19	40.56	0.228	40.56	3.38 ± 6.4	0	40.38	2.38 ± 3.73	0.007	25.29	0.128
Yes	40.5	4.75 ± 5.98	0.62	29.23	0.007	29.23	4.75 ± 7.02	0.51	27.6	2 ± 3.28	0.013	15.84	0.128
ER expression													
Negative	33.6	5.82 ± 8.12	0.74	40.56	0.007	40.56	6.42 ± 9.4	0.74	40.38	3.09 ± 5.33	0.02	25.29	0.846
Positive	66.4	2.96 ± 4.16	0.19	29.23	0.007	29.23	2.59 ± 4.07	0	27.6	1.87 ± 2.4	0.007	11.39	0.846
PR expression													
Negative	41.4	5.24 ± 7.47	0.19	40.56	0.0302	40.56	5.67 ± 8.66	0	40.38	2.33 ± 3.38	0.019	15.84	0.939
Positive	58.6	2.99 ± 4.38	0.54	29.23	0.0302	29.23	2.62 ± 4.28	0.51	27.6	2.18 ± 3.68	0.007	25.29	0.939
Her2 expression													
Negative	75.9	3.16 ± 5.42	0.19	40.56	0.0052	40.56	2.87 ± 5.52	0	40.38	2.25 ± 2.89	0.02	15.84	0.939
Positive	24.1	6.46 ± 6.98	1.03	29.23	0.0052	29.23	7.25 ± 8.69	0.83	27.6	2.19 ± 5.47	0.007	25.29	0.939
Tumor size													
T1 ≤ 2 cm	19.8	3.9 ± 5.18	0.8	23.67	0.001	23.67	3.87 ± 6.31	0.66	24.64	2.91 ± 5.29	0.019	25.29	0.56
2 < T2 ≤ 5 cm	55.2	2.85 ± 3.19	0.19	19.41	0.001	19.41	2.63 ± 3.55	0	19.19	1.82 ± 2.7	0.007	11.39	0.56

Table 2 (continued)

Variable	N (%)	Mean Methylation			p value	Sub_mean Methylation			p value	mRNA expression (2 ^{ΔΔCt})			p value
		Mean±SD	Min	Max		Mean±SD	Min	Max		Mean±SD	Min	Max	
T3 > 5 cm	11.2	3.32±4.42	0.54	17.76		3.57±5.72	0.73	22.45		3.15±4.42	0.06	15.84	
T4	13.8	8.76±11.55	0.72	40.56		9.26±12.27	0.66	40.38		2.22±2.3	0.06	7.95	
Lymphnode status					0.79				4.52E-01				0.68
N0	44	4.03±7.07	0.54	40.56		3.86±7.44	0.51	40.38		2.56±4.33	0.007	25.29	
N1	31	3.69±5.18	0.19	29.23		3.45±5.27	0	27.6		1.78±2.07	0.01	7.95	
N2	17.2	3.42±4.69	0.72	17.76		3.55±6.14	0.66	22.45		2.39±3.41	0.02	11.39	
N3	7.8	5.62±4.43	0.93	14.85		6.79±7.46	0.7	24.68		0.93±1.07	0.05	2.72	
Metastasis					0.0969				6.88E-02				0.378
M0	88.6	3.52±5.54	0.19	40.56		3.35±6.02	0	40.37		2.34±3.72	0.007	25.29	
M1	11.4	6.21±8.06	0.93	29.23		6.34±8.55	0.7	27.6		1.28±1.45	0.02	4.63	
TNM stage					0.264				1.41E-01				0.75
I	14.9	3.36±5.36	0.8	23.67		2.96±5.1	0.66	22.49		3.22±5.81	0.09	25.29	
IIA	26.3	3.09±3.65	0.62	19.41		2.75±3.83	0.51	19.19		1.73±2.34	0.007	7.56	
IIB	21.9	2.86±3.12	0.19	14.17		2.75±3.71	0	17.13		2.15±3.51	0.01	15.84	
IIIA	13.2	3.08±3.99	0.77	17.76		3.02±5.21	0.88	22.45		3.07±3.75	0.02	11.39	
IIIB	9.7	6.76±11.85	0.72	40.56		7.1±12.7	0.66	40.38		2.24±4.42	0.06	7.95	
IIIC	2.6	3.95±1.68	1.62	5.56		3.98±2.63	1.38	7.59		0.2±0	0.2	0.2	
IV	11.4	6.21±8.06	0.93	29.23		6.34±8.55	0.7	27.6		1.28±1.45	0.02	4.63	
NK-TILs					0.081				0.0682				0.719
High	78.8	3.25±5.38	0.19	40.56		3.1±5.9	0	40.38		2.3±3.97	0.028	25.29	
Low	21.2	3.32±6.38	0.77	23.67		5.42±6.94	0.88	22.49		1.94±2.19	0.007	6.17	
TILs					0.596				8.63E-01				0.765
Low	53.5	3.45±4.95	0.54	29.23		3.47±5.56	0.51	27.6		2.67±4.4	0.02	25.29	
Moderate	28.1	4.65±7.7	0.62	40.56		4.05±7.6	0.7	40.38		1.81±2.56	0.007	10.67	
High	18.4	3.83±5.3	0.19	19.44		4.05±6.63	0	26.11		1.79±1.82	0.09	5.49	

Bold numbers indicate statistically significant correlations with p values less than 0.05

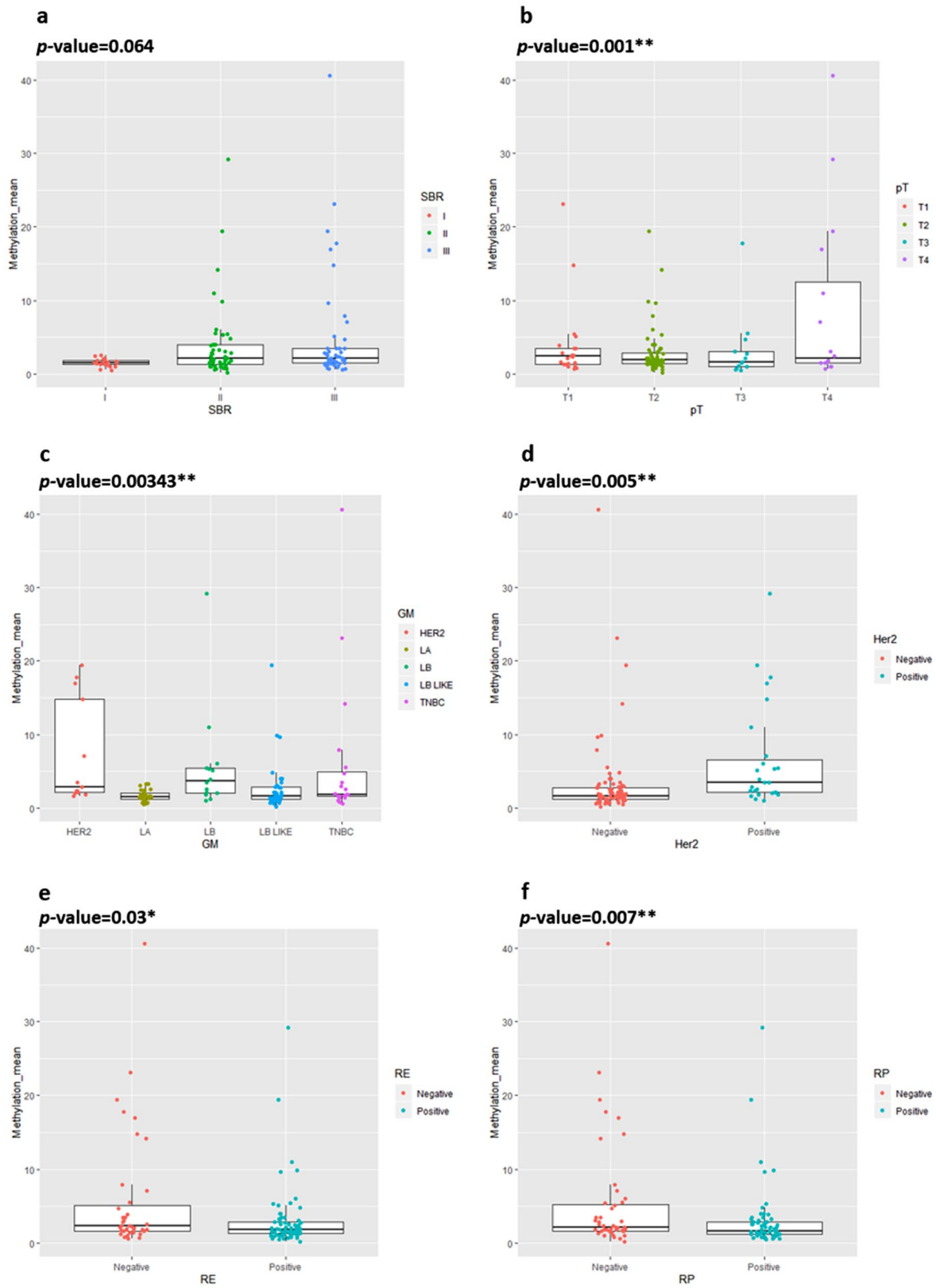


Fig. 2 CD155 promoter methylation mean according to clinical-pathological features. The x-axis shows the mean percentage of global methylation and y-axis shows **a** SBR grade, **b** Tumor size, **c** Molecular group, **d** Her2 receptor, **e** RE receptor, **f** RP receptor

Table 3 Associations between individual CpG sites and clinical-pathological indicators

Variable	CpG1	CpG2	CpG3	CpG4	CpG5	CpG6	CpG7	CpG8	CpG9	CpG10	CpG11	CpG12	CpG13	CpG14
<i>P values</i>														
SBR grade	0.095	0.1	0.19	0.15	1.05e-1	7.08e-2	2.17e-2	0.103	2.46e-2	0.132	0.06	0.130	0.07	0.16
GM	0.0338	0.0575	0.0171	0.00215	0.000332	0.0000679	5.60e-5	0.00518	8.75e-6	0.0329	0.237	0.0383	0.0117	0.09
Histological type	0.713	0.974	0.373	0.376	5.32e-1	8.22e-1	7.97e-1	0.588	9.21e-1	0.450	0.786	0.610	0.904	0.580
Invasion	0.277	0.0469	0.429	0.220	2.85e-1	2.74e-1	1.18e-1	0.37	1.58e-1	0.418	0.239	0.361	0.326	0.841
HER2	0.0582	0.0291	0.0279	0.000899	0.000917	0.000140	8.85e-4	0.00721	2.33e-4	0.0141	0.103	0.172	0.0267	0.158
RE	0.0305	0.106	0.0452	0.0118	0.00107	0.000611	1.70e-4	0.00908	5.28e-5	0.0590	0.228	0.0535	0.00784	0.185
RP	0.77	0.231	0.104	0.0377	0.00645	0.00414	2.07e-3	0.0331	5.46e-4	0.143	0.389	0.113	0.0342	0.321
pT	0.00201	0.0177	0.00569	0.000399	2.16e-4	8.64e-4	9.55e-4	0.00154	3.64e-4	0.000984	0.0375	0.0315	0.00686	0.0200
pN	0.788	0.956	0.856	0.535	3.55e-1	6.98e-1	2.00e-1	0.679	3.16e-1	0.718	0.990	0.872	0.857	0.72
Metastasis	0.100	0.141	0.267	0.0434	0.0617	0.0706	1.01e-1	0.180	5.24e-2	0.0643	0.180	0.390	0.156	0.277
TNM stage	0.27	0.534	0.363	0.130	8.91e-2	1.91e-1	1.28e-1	0.241	1.27e-1	0.199	0.717	0.645	0.356	0.581

Abbreviations: SBR, Scarff-Bloom-Richardson; GM, Molecular Group; pT, Tumor Size; pN, Lymphnode status; TNM, tumor-node-metastasis; Her2, human epidermal growth factor receptor 2; RE, estrogen receptor; PR, Progesterone receptor

Bold numbers indicate statistically significant correlations with *p* values less than 0.05

CpG9 and CpG11 sites (p value = 3.53e-2, p value = 0.0347, p value = 1.39e-2 and p value = 0.0119, respectively), where we noted a correlation between a higher methylated status and a dense infiltrate of NK-TILs (Fig. 3a–d).

These results showed that the methylation percentages of CpG4 to CpG9 sites were better suited to be associated with clinical-pathological parameters than the average global CD155 methylation percentage. Therefore, CpG4 to CpG9 sites mean percentage methylation was used in the subsequent analyses. Thus, all analyses were performed with the average (sub_mean) of CD155 methylation over all six CpGs (CpG4 to CpG9), and this did not affect the general conclusions (Table 2).

CD155 membranous mRNA isoform expression analysis

We studied the expression profile of CD155 by quantitative real-time PCR. We already highlighted that CD155 is expressed in several isoforms corresponding to splicing variants, it is expressed at the cytoplasmic or membrane level, this localization is tightly related to these isoforms. In fact, CD155 undergoes alternative splicing, generating four unique splicing isoforms. It can be expressed in a soluble form lacking a transmembrane domain, encoded by alternative splice isoforms β and γ , or as a membrane-bound protein encoded by two alternative splicing isoforms, α and δ . To analyze the relative expression of CD155 transcripts, we designed a primer set which amplifies cDNA but not genomic DNA. This primer set amplifies the sequence that covers the transmembrane domain, one primer of this set is located on exon 6 which corresponds to the transmembrane domain (α isoform), while the other is located on the junction exon 6–exon 7. CD155 transcripts were detected in most patients, although at different levels. The relative expression of each gene was normalized with respect to the housekeeping gene β -Actin (ACTB). The overall transcriptome patterns displayed a similar distribution of the normalized intensity values among all samples with no significant differences between the affected and control groups (p value = 0.50). Relative mRNA abundance was determined by the $2^{-\Delta\Delta Cq}$ method ($\Delta\Delta Cq_x$: [Cq_x gene test – Cq_x endogenous control] – mean of ΔCq healthy control), and results are summarized as the mean \pm s.d of two independent experiments. Correlations of CD155 mRNA expression profile with clinical indicators are summarized in Table 2. The only significant association was observed with histological type (p value = 0.045).

Correlations between DNA hypomethylation variations and transcriptional expression data

CD155 mRNA transcripts were analyzed to verify possible associations with global changes in DNA methylation

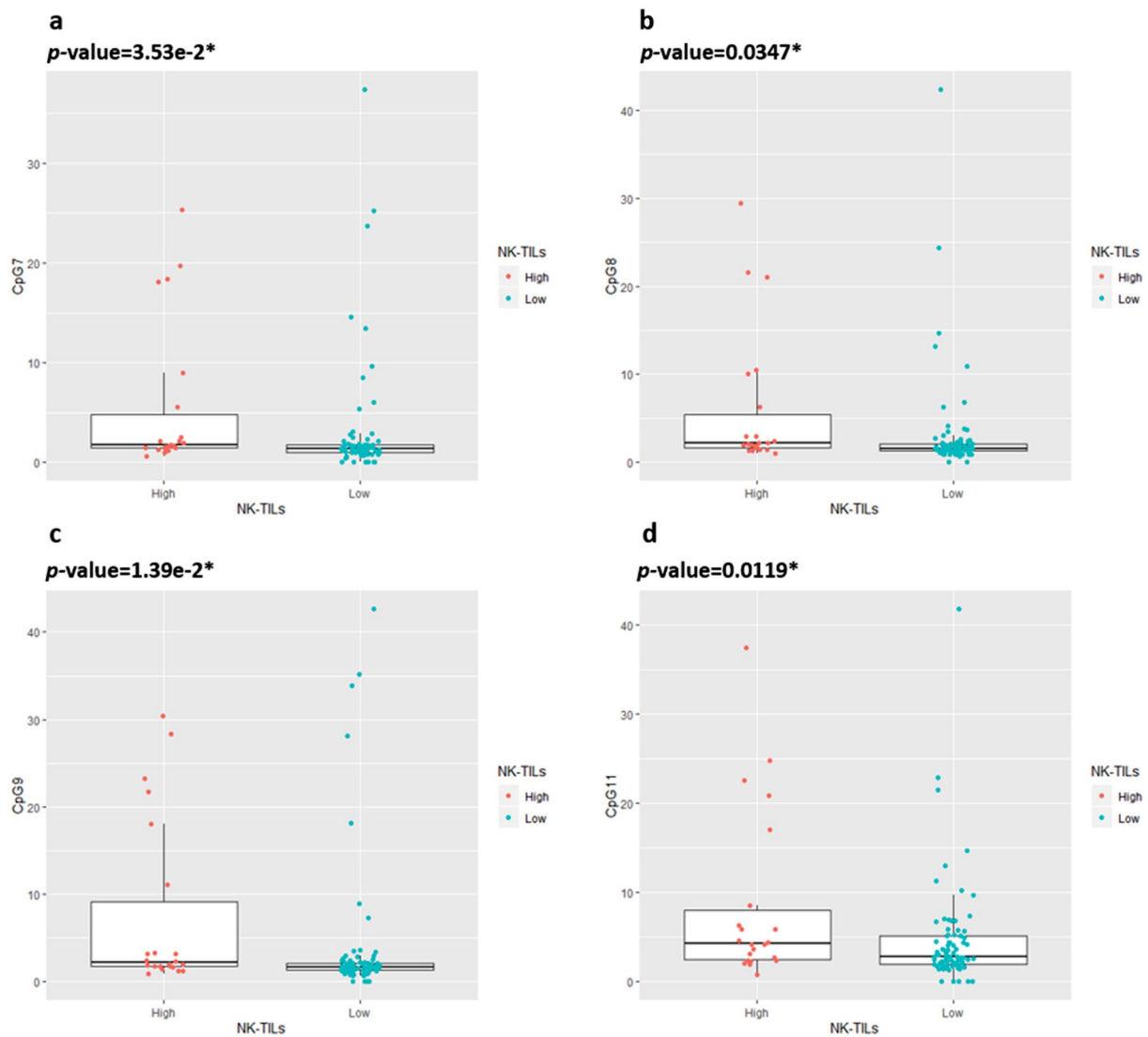


Fig. 3 CD155 promoter methylation percentage of individual CpGs sites according to NK-TILs. The x-axis shows the methylation percentage of a CpG7, b CpG8, c CpG9 and d CpG11 sites and y-axis shows NK-TILs

levels (sub_mean methylation percentage) for each patient. Samples lacking DNA methylation revealed relatively higher trend of CD155 transcription levels though not statistically significant (p value: 0.370, Fig. 4a). Consistent with these results, patients with strongest transcription levels for this checkpoint molecule were highly hypomethylated, when methylation was dichotomized according to its median into highly or weakly hypomethylated tumors (p value = 0.159, Fig. 4b).

Altogether, association between methylation and transcription levels for this gene was found insignificant, suggesting that CD155 expression might not be exclusively regulated by DNA methylation.

Correlations between CD155 membranous mRNA isoform expression and protein localization

We have earlier reported CD155 protein expression as strong prognostic parameter that is associated with breast cancer progression and patient's outcome. Beforehand, we characterized two protein localizations via an immunohistochemistry detection method (IHC), which showed different contributions of each isoform in BC progression [14]. This prompted us to investigate potential correlations between CD155 membranous mRNA isoform expression and protein localization. Therefore, we attempted to confirm whether CD155 membranous mRNA isoform expression is

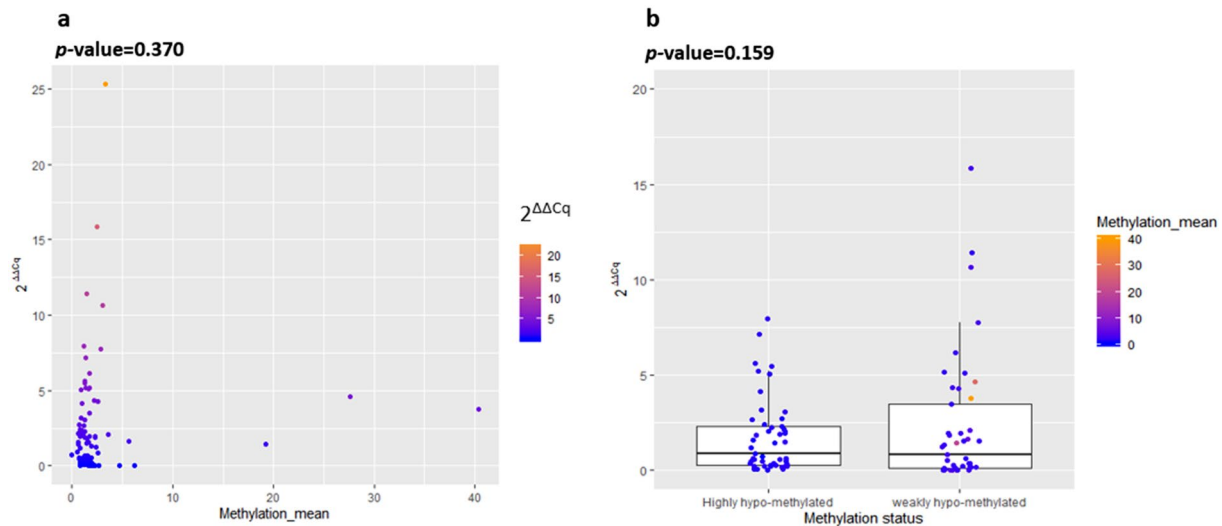


Fig. 4 Different DNA methylation patterns for CD155 with respect to transcription levels **a** Distribution of methylation mean percentage across six CpG sites and **b** methylation dichotomized according to its

median into highly or weakly hypomethylated tumors according to CD155 membranous mRNA isoform expression ($2^{\Delta\Delta Cq}$)

related to protein localization. To this end, we assessed the correlations between CD155 mRNA expression levels and CD155 protein expression. Despite the limited statistical significance, our results suggest that CD155 membranous mRNA isoform expression is positively related to membranous CD155 (m-CD155) protein localization, where high m-CD155 protein expression tumors reveal high transcription levels which are clearly reduced in tumors with high cytoplasmic CD155 protein expression (cyt-CD155). Although there was no significant correlation with

transcription levels for both protein localizations, Fig. 5a, b shows a clear reciprocal trend, although with poor statistical significance.

CD155 promoter methylation impact on patient's outcome

Overall survival (OS) and disease-free survival (DFS) were investigated by survival analysis over a 5-year period. Cox proportional hazard analyses were performed to determine

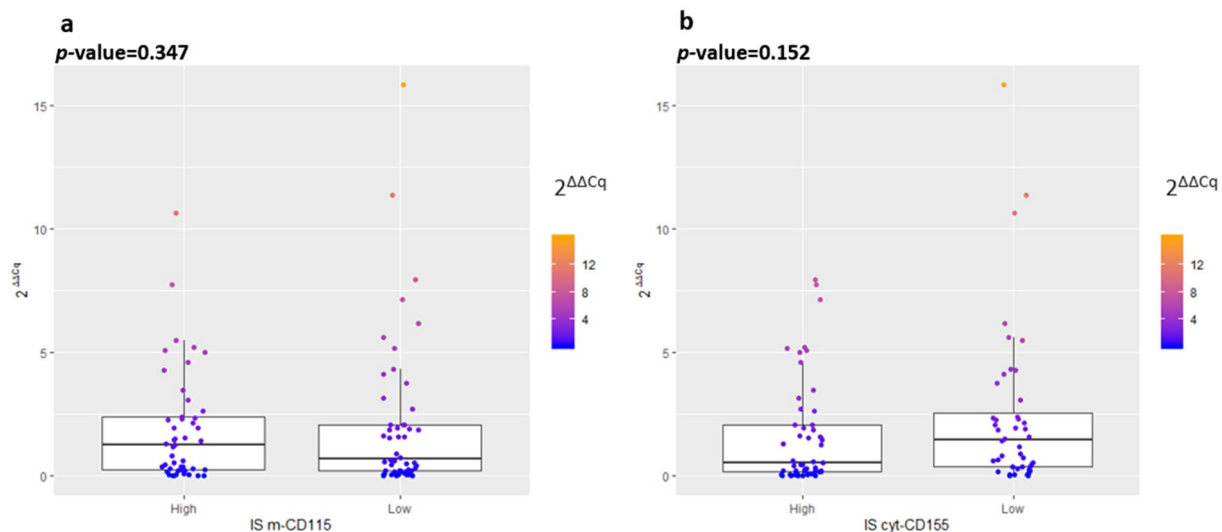


Fig. 5 Correlations between CD155 membranous mRNA isoform expression analyzed by RT-qPCR and protein localization determined by IHC. Boxplot representation showing a comparison of **a** m-CD155

and **b** cyt-CD155 distribution with respect to CD155 membranous isoform transcription levels ($2^{\Delta\Delta Cq}$)

the prognostic value of CD155 overall methylation mean and CpG4- > CpG9 average methylation (sub_mean) in breast cancer patients.

Cox proportional hazard models were fit to estimate the effect of the non-dichotomized CD155 global methylation mean and CpG4- > CpG9 average methylation percentages, accounting for tissue type. A significant association between CD155 global methylation mean or CpG4- > CpG9 average methylation and overall survival could be confirmed. The trend toward a negative effect of methylation percentage on patient survival was observed. In univariate Cox proportional hazard analysis, increased CD155 global methylation mean percentage (Hazard ratio [HR] = 1.051, 95% confidence interval (CI) = 1.010 to 1.095, p value = 0.015) or sub_mean methylation percentage (HR = 1.044, 95% CI = 1.003 to 1.087, p value = 0.033) was significantly associated with reduced OS. Changes in DNA methylation at specific CpG sites showed a significant correlation between increased methylation at CpG7 individual site and reduced overall survival (HR = 1.049, 95% CI = 1.007 to 1.094, p value = 0.023).

Multivariate Cox proportional hazard analyses including SBR grade, molecular group, tumor size, distant metastasis, TILs and NK-TILs infiltration, and the expression of both cytoplasmic and membranous CD155 protein added significant prognostic information with regard to OS and DFS for CD155 global methylation mean percentage (HR = 1.106, 95% CI = 1.038 to 1.177, p value = 0.002 for OS; HR = 1.064, 95% CI = 1.008 to 1.122, p value = 0.024 for DFS) or CpG4- > CpG9 average methylation percentage (HR = 1.097, 95% CI = 1.031 to 1.167, p value = 0.003 for OS; HR = 1.059, 95% CI = 1.004 to 1.116, p value = 0.036 for DFS). These results confirm that CD155 methylation is an independent predictor of survival.

Since CD155 mRNA expression and DNA methylation seem to be related, we next sought to determine their value in predicting clinical outcome. Multivariate analysis further confirmed that CD155 methylation is an independent risk factor for breast cancer patients. The impact of other covariates (adjustment factors), including CD155 membranous mRNA isoform expression, SBR grade, molecular group, tumor size, metastasis, TILs and NK-TILs infiltration, and the expression m-CD155 and cyt-CD155 protein on overall survival and disease-free survival, was tested and showed a significant and unfavorable effect of CpG4- > CpG9 average methylation percentage (sub_mean) on survival (HR = 1.103, 95% CI = 1.024 to 1.187, p value = 0.010 for OS; HR = 1.059, 95% CI = 1.001 to 1.121, p value = 0.048 for DFS). Furthermore, the prognostic value of CD155 membranous mRNA isoform expression on OS was also verified in the combined analysis, and the results showed that lower expression pointed to poorest overall survival (HR = 0.874, 95% CI = 0.712 to 1.074). In addition, the

impacts of CD155 membranous mRNA isoform expression and m-CD155 protein expression on patient's outcome are consistent (HR = 0.472, 95% CI = 0.132 to 1.691).

Discussion

Breast cancer is known to be one of the most complex, multi-factorial and multi-signal biological process in carcinogenesis. Gene mutations and epigenetic modifications are factors resulting in tumorigenesis and cancer progression of breast tumors. Besides, aberrant DNA methylation patterns are associated with transcriptional repression, abnormal activation or inactivation of signaling pathways, abnormal apoptotic mechanisms, activation of proto-oncogenes and the promotion of tumorigenesis. One of the most attractive routes is the panel of immune checkpoint molecules which seems to have an important role in the physiopathology of cancers. Among these molecules, CD155 expression has been recently described with its pivotal function in a wide range of malignant cancers due to its complex interactions and associated roles in the immune response [8–11, 14, 31]. More specifically, we have previously reported the differential contribution of CD155 protein expression according to its localization site in breast cancer progression and outcome. We provided evidence that CD155 is expressed at the cytoplasmic or membranous level, thereby differential localization seems to have an importance in the tumor microenvironment designing and physio-pathological features [14]. Interestingly, CD155 gene transcription leads to mRNA products that can be alternatively spliced into different isoforms and ultimately translated in four possible proteins, two transmembrane forms and two soluble forms [17]. For this, we have hypothesized an epigenetic regulation, we precisely speculate changes in methylation status of CD155 gene. In this study, we have evaluated the potential use of CD155 promoter methylation as a prognostic biomarker in breast cancer. DNA methylation changes were validated by pyrosequencing, the targeted region in our study contains 14 specific CpGs sites in the promoter region of CD155 gene.

We tempted to elucidate whether CD155 expression is under direct epigenetic control in breast cancer patients. Indeed, transcriptional analyses were carried out in order to ascertain if hypomethylation variations would affect CD155mRNA expression. Our results showed consistent patterns where trends were consistently negative for all CpG sites. Thus, we observed higher but not statistically significant CD155 membranous mRNA isoform transcription levels among samples lacking DNA methylation. Previously, many studies have reported that gene expression is a complex process and that the interplay between many different genetic, epigenetic, and epi-transcriptomic factors may also be involved in regulation of gene expression [32–34].

Besides, differences in methylation levels might be necessary but not sufficient for genes expression. Our data seem to point into the same direction; thus, this might explain the lack of significant association between CD155 methylation and mRNA expression. Further, in order to clarify the interplay between protein and mRNA expression, we aimed to confirm whether CD155 membranous mRNA isoform expression is related to protein localization. Our results showed a positive association between CD155 membranous mRNA isoform overexpression and high membranous CD155 (m-CD155) protein localization. The consistency between CD155 mRNA isoform expression and protein localization suggests that the expression of m-CD155 protein reflects the transcription of the corresponding isoform and is likely to be regulated at the transcriptional level in breast cancer tissues. This conclusion is supported by previous study showing the relationship between gene expression measured at the mRNA level and the corresponding protein level in lung adenocarcinomas [35].

Our results identify for the first time that the CD155 promoter methylation pattern is a reliable clinicopathological biomarker of immune checkpoint regulation in solid tumors. Previous studies have only shown the expression of CD155 by cancer cells but no study has reported its promoter methylation status. Herein, we have initially described the clinical impact of CD155 promoter methylation pattern. Statistical analyses demonstrated that higher levels of CD155 promoter methylation correlated with higher tumor size. In agreement with this observation, previous studies reported that CD155 expression level was significantly associated with tumor size in breast cancer, soft tissue sarcoma and in primary small cell carcinoma of the esophagus [36], 37, 38. Further, CD155 methylation levels among molecular subgroups showed significant results, most importantly, the Her2, LB and TNBC groups correlated with higher methylation rates. In contrast, recent studies reported that the proportion of patients with CD155 expression was higher in TNBC compared to LA groups [15, 39]. Our conclusion does not differ from previous reports as methylation rates in our study remain relatively low. In addition, we identified a strong and positive correlation between a higher methylation percentage and the expression of the HER2 receptor. Meanwhile, negative correlations with progesterone and estrogen receptors expression status were identified. Thus, on the basis of data obtained from the publicly available database from The Cancer Genome Atlas (TCGA), we compared clinical DNA methylation data from the TCGA with differentially methylated DNA within the targeted CpG motifs in CD155 gene promoter, and we obtained similar conclusions. In fact, CD155 expression and its promoter methylation status are negatively correlated, which is confirmed by the Pearson correlation coefficients. Besides, a comprehensive study by the TCGA Network [40, 41] has demonstrated clear

differences in CD155 expression and methylation, as well as HER2, estrogen and progesterone receptor status, and molecular subtypes between the different breast cancer samples.

Moreover, when comparing patient's distant metastasis and lymphovascular invasion according to CD155 promoter methylation or protein expression in breast cancer tissues, data show a limited significant but interesting association between no distant metastasis or lymphovascular invasion and CD155 promoter methylation and with loss of m-CD155 protein expression in breast cancer tissues as we previously reported [14]. Our results clearly show that CD155 promoter methylation correlated with CD155 protein expression and the invasion process implying that methylation of the CD155 promoter may affect tumor progression in advanced breast cancer tissues via the regulation of protein expression at the membranous localization. This may be due to changes in the tumor microenvironment resulting from CD155 aberrant methylation. Further studies investigating the mechanism behind this process may offer insights into potential therapeutic targets or prognostic biomarkers in breast cancer disease monitoring. Indeed, checkpoint inhibitors have become an efficient way for cancer therapy. Notably, monoclonal antibodies targeting the PD-1/PD-L1 signaling axis have shown striking clinical success against multiple malignancies. However, while these therapies are very efficient in certain tumors, others showed low response rates to PD-1/PD-L1 blockade [42]. This discrepancy might be explained by the immune infiltrate, the differential expression status of target molecules, and the impact of the tumor microenvironment. Interestingly, CD155, which interacts with receptors expressed on T and NK cells, recently emerged as a compelling immunotherapeutic target [43, 44]. CD155 has an immunoregulatory potential upon interaction with DNAM-1, CD96, and TIGIT, resulting in two distinct profiles of effector cell activation. In the setting of cancer, TIGIT is under active investigation as a target for immune checkpoint blockade owing to its inhibitory effects on T cell proliferation and function [45]. In preclinical models, it was recently reported that TIGIT blockade has limited efficacy as a monotherapy but is able to significantly potentiate the efficacy of PD-1 and CD96 blockade [46]. It was demonstrated that TIGIT/PD-1 is expressed on CD8+ lymphocytes, suggesting that cancerous cells may be able to upregulate PD-L1 and CD155 during immune evasion, by interacting with their ligands expressed on TILs to suppress their cytotoxic activities. Additionally, CD155 overexpression on malignant epithelium in high-grade serous ovarian cancer suggests that the disease may be subject to therapeutic strategies targeting CD155, such as oncolytic poliovirus, which is showing promising results in phase I trials against malignant glioma [43]. Finally, it was demonstrated that CD155/PVR is commonly expressed in TILs negative tumors suggesting that

targeting the CD155/TIGIT pathway might prove complementary to PD-1/PD-L1-directed approaches [46]. The deeper mechanisms underlying this relationship deserve further exploration, and more particularly the significance of CD155 promoter methylation status in immunotherapy.

To further evaluate CD155 influence upon patient prognosis, multivariate analyses were conducted and showed that decreased CD155 methylation mean percentage is significantly associated with better patients' survival, which clearly reflects an unfavorable prognosis of CD155 methylation. It has been largely demonstrated that CD155 has a pivotal role in a broad range of malignant tumors. A recent study reported that overexpression of CD155 in cancer cells correlated with an unfavorable prognosis of patients with lung adenocarcinoma [31], another study demonstrated that patients with pancreatic cancer displaying higher CD155 expression levels had significantly poor prognosis [11]. Likewise, upregulated CD155 expression correlated with aggressive clinical-pathological features and unfavorable prognosis in patients with cholangiocarcinoma [47] and with primary small cell carcinoma of the esophagus [38]. While these previous studies reported that CD155 expression was a poor prognostic marker, other studies reported opposite results. Thus, studies on breast carcinoma and hepatocellular carcinoma showed that tumors overexpressing CD155 correlated with good prognosis [14, 48]. These discrepancies suggest that CD155 may serve dual functions owing to its immunological and non-immunological mechanisms in various types of human cancers. Our finding is in good agreement with previous studies showing that the expression of CD155 is positively correlated with good prognosis in breast cancer and hepatocellular carcinoma [14, 48]. Our results showed consistency with m-CD155 protein expression findings and further elucidated that CD155 methylation is an independent predictor of prognosis. With the analysis above, we believe that CD155 methylation may be a prospective biomarker to predict the prognosis of breast cancer patients. Taken together, we speculate CD155 methylation as a potential regulator of CD155 expression and as an independent predictor of overall survival and disease-free survival in breast cancer patients.

Conclusion

Data generated in our study provide more evidence in respect to the identification of new reliable epigenetic biomarkers which is important in achieving a better prognosis. To date, CD155 immune checkpoint methylation has not been analyzed in breast cancer or any type of cancer. Our study suggests that quantification of CD155 promoter methylation levels by pyrosequencing is a promising diagnostic biomarker assay approach to predict breast tumor

evolution and prognosis. Specifically, we identified six CpGs sites in CD155 gene promoter which perform well compared to the global methylation of all 14 CpGs. Hence, combining CD155 CpG4→CpG9 methylation rates could improve its sensitivity to correlate with clinical-pathological parameters and disease outcome. One of the intriguing findings of our study is that single CpG site 7 showed significant correlations with NK cell infiltrate, clinical parameters and prognosis. The level of methylation at this site deserves confirmation for therapeutic approaches as a potential target. Thus, further research on the role of CD155 methylation would be of considerable interest and will certainly add to our understanding of the regulation of gene products.

Acknowledgements We thank our study participants for their contribution to this study. A further thanks goes to the Protein Chemistry, Proteomics and Epigenetic Signaling (PPES), University of Antwerp, team members for their collaboration and valuable contribution. This work was partially supported by ISESCO (Islamic Educational, Scientific and Cultural Organization) Research grant (Ref No. 2148).

Author contributions HT contributed to data curation, formal analysis, investigation, methodology, software, validation, visualization, writing—original draft, writing—review and editing. KD contributed to formal analysis, software, visualization. SC contributed to data curation, project administration, resources, supervision, validation. KC contributed to data curation, resources. SBH contributed to data curation, resources. WBK contributed to data curation, resources. TS contributed to data curation, resources. AR contributed to formal analysis, project administration, supervision, validation. WVVB contributed to project administration, resources, supervision, validation, visualization, writing—review and editing. BC contributed to conceptualization, funding acquisition, investigation, methodology, project administration, resources, supervision, validation, visualization, writing—review and editing.

Funding This work was financially supported by ISESCO (Islamic Educational, Scientific and Cultural Organization) Research grant (Ref N°2148).

Availability of data and material All data generated or analyzed during this study are included in this published article.

Declarations

Conflicts of interest The authors have no conflicts of interest to declare.

Ethics approval All procedures performed in studies involving human participants were in accordance with the ethical standards of the institutional and the national research committee of Habib Bourguiba University Hospital and with the 1964 Helsinki declaration and its later amendments or comparable ethical standards. Sampling was made only on patient tissues from tissue library of Pathology Department-Habib Bourguiba Hospital, and no samples were made specifically for the study.

Consent to participate We have conducted a retrospective study, for this type of study, formal consent is not required.

Consent for publication All authors reviewed and approved the manuscript for submission.

References

- Pardoll DM (2012) The blockade of immune checkpoints in cancer immunotherapy. *Nat Rev Cancer* 12(4):252–264. <https://doi.org/10.1038/nrc3239>
- Topalian SL, Drake CG, Pardoll DM (2015) Immune checkpoint blockade: a common denominator approach to cancer therapy. *Cancer Cell* 27(4):450–461. <https://doi.org/10.1016/j.ccell.2015.03.001>
- Sharma P, Allison JP (2015) The future of immune checkpoint therapy. *Science* 348(6230):56–61. <https://doi.org/10.1126/science.aaa8172>
- Chaudhary B, Elkord E (2016) Regulatory T Cells in the Tumor Microenvironment and Cancer Progression: Role and Therapeutic Targeting. *Vaccines* (Basel). <https://doi.org/10.3390/vaccines4030028>
- Sasidharan Nair V, Elkord E (2018) Immune checkpoint inhibitors in cancer therapy: a focus on T-regulatory cells. *Immunol Cell Biol* 96(1):21–33. <https://doi.org/10.1111/imcb.1003>
- Dougall WC, Kurtulus S, Smyth MJ, Anderson AC (2017) TIGIT and CD96: new checkpoint receptor targets for cancer immunotherapy. *Immunol Rev* 276(1):112–120. <https://doi.org/10.1111/imr.12518>
- Chan CJ et al (2014) The receptors CD96 and CD226 oppose each other in the regulation of natural killer cell functions. *Nat Immunol* 15(5):431–438. <https://doi.org/10.1038/ni.2850>
- Masson D et al (2001) Overexpression of the CD155 gene in human colorectal carcinoma. *Gut* 49(2):236–240
- Nakai R et al (2010) Overexpression of Necl-5 correlates with unfavorable prognosis in patients with lung adenocarcinoma. *Cancer Sci* 101(5):1326–1330. <https://doi.org/10.1111/j.1349-7006.2010.01530.x>
- Bevelacqua V et al (2012) Nectin like-5 overexpression correlates with the malignant phenotype in cutaneous melanoma. *Oncotarget* 3(8):882–892. <https://doi.org/10.18632/oncotarget.594>
- Nishiwada S et al (2015) Clinical significance of CD155 expression in human pancreatic cancer. *Anticancer Res* 35(4):2287–2297
- Sloan KE, Stewart JK, Treloar AF, Matthews RT, Jay DG (2005) CD155/PVR enhances glioma cell dispersal by regulating adhesion signaling and focal adhesion dynamics. *Cancer Res* 65(23):10930–10937. <https://doi.org/10.1158/0008-5472.CAN-05-1890>
- Stamm H et al (2019) Targeting the TIGIT-PVR immune checkpoint axis as novel therapeutic option in breast cancer. *Oncoimmunology* 8(12):e1674605. <https://doi.org/10.1080/2162402X.2019.1674605>
- Triki H et al (2019) CD155 expression in human breast cancer: Clinical significance and relevance to natural killer cell infiltration. *Life Sci* 231:116543. <https://doi.org/10.1016/j.lfs.2019.116543>
- Y.-C. Li et al., (2020) Overexpression of an Immune Checkpoint (CD155) in Breast Cancer Associated with Prognostic Significance and Exhausted Tumor-Infiltrating Lymphocytes: A Cohort Study. *Journal of Immunology Research*. <https://www.hindawi.com/journals/jir/2020/3948928/>. Accessed 08 Apr 2020
- Excoffon KJDA, Bowers JR, Sharma P (2014) 1. Alternative splicing of viral receptors: A review of the diverse morphologies and physiologies of adenoviral receptors. *Recent Res Dev Virol* 9:1–24
- Koike S et al (1990) The poliovirus receptor protein is produced both as membrane-bound and secreted forms. *EMBO J* 9(10):3217–3224
- Béatrice B et al (2003) Identification of secreted CD155 isoforms. *BiochemBiophys Res Commun*. 309(1):175–182. [https://doi.org/10.1016/s0006-291x\(03\)01560-2](https://doi.org/10.1016/s0006-291x(03)01560-2)
- Lozano E, Dominguez-Villar M, Kuchroo V, Hafler DA (2012) The TIGIT/CD226 axis regulates human T cell function. *J Immunol* 188(8):3869–3875. <https://doi.org/10.4049/jimmunol.1103627>
- Kulis M, Esteller M (2010) DNA methylation and cancer. *Adv Genet* 70:27–56. <https://doi.org/10.1016/B978-0-12-380866-0.60002-2>
- Sinčić N, Herceg Z (2011) DNA methylation and cancer: ghosts and angels above the genes. *Curr Opin Oncol* 23(1):69–76. <https://doi.org/10.1097/CCO.0b013e3283412eb4>
- Wu Y, Sarkissyan M, Vadgama JV (2015) Epigenetics in breast and prostate cancer. *Methods Mol Biol* 1238:425–466. https://doi.org/10.1007/978-1-4939-1804-1_23
- Sasidharan Nair V, El Salhat H, Taha RZ, John A, Ali BR, Elkord E (2018) DNA methylation and repressive H3K9 and H3K27 trimethylation in the promoter regions of PD-1, CTLA-4, TIM-3, LAG-3, TIGIT, and PD-L1 genes in human primary breast cancer. *Clin Epigenetics*. <https://doi.org/10.1186/s13148-018-0512-1>
- Roulois D, Yau HL, De Carvalho DD (2016) Pharmacological DNA demethylation: Implications for cancer immunotherapy. *Oncoimmunology* 5(3):e1090077. <https://doi.org/10.1080/2162402X.2015.1090077>
- Maruvada P, Wang W, Wagner PD, Srivastava S (2005) Biomarkers in molecular medicine: cancer detection and diagnosis. *Bio-techniques*. <https://doi.org/10.2144/05384su04>
- Wolff AC et al (2013) Recommendations for human epidermal growth factor receptor 2 testing in breast cancer: American Society of Clinical Oncology/College of American Pathologists clinical practice guideline update. *J Clin Oncol* 31(31):3997–4013. <https://doi.org/10.1200/JCO.2013.50.9984>
- Bouziidi L et al (2021) Prognostic value of natural killer cells besides tumor infiltrating lymphocytes in breast cancer tissues. *Clin Breast Cancer*. <https://doi.org/10.1016/j.clbc.2021.02.003>
- Sambrook J, Russell DW (2006) Purification of nucleic acids by extraction with phenol:chloroform. *CSH Protoc*. 2006(1):169–170. <https://doi.org/10.1101/pdb.prot4455>
- Saiki RK et al (1988) Primer-directed enzymatic amplification of DNA with a thermostable DNA polymerase. *Science* 239(4839):487–491
- Declerck K et al (2017) Interaction between prenatal pesticide exposure and a common polymorphism in the PON1 gene on DNA methylation in genes associated with cardio-metabolic disease risk—an exploratory study. *Clin Epigenetics*. <https://doi.org/10.1186/s13148-017-0336-4>
- Sun Y et al (2020) Combined evaluation of the expression status of CD155 and TIGIT plays an important role in the prognosis of LUAD (lung adenocarcinoma). *Int Immunopharmacol* 80:106198. <https://doi.org/10.1016/j.intimp.2020.106198>
- Jones PA, Baylin SB (2007) The epigenomics of cancer. *Cell* 128(4):683–692. <https://doi.org/10.1016/j.cell.2007.01.029>
- Jones PA (2012) Functions of DNA methylation: islands, start sites, gene bodies and beyond. *Nat Rev Genet* 13(7):484–492. <https://doi.org/10.1038/nrg3230>
- Gibney ER, Nolan CM (2010) Epigenetics and gene expression. *Heredity*. <https://doi.org/10.1038/hdy.2010.54>
- Chen G et al (2002) Discordant protein and mRNA expression in lung adenocarcinomas. *Mol Cell Proteomics* 1(4):304–313. <https://doi.org/10.1074/mcp.M200008-MCP200>
- Yong H et al (2019) CD155 expression and its prognostic value in postoperative patients with breast cancer. *Biomed Pharmacother* 115:108884. <https://doi.org/10.1016/j.biopha.2019.108884>

37. Atsumi S, Matsumine A, Toyoda H, Niimi R, Iino T, Sudo A (2013) Prognostic significance of CD155 mRNA expression in soft tissue sarcomas. *Oncol Lett* 5(6):1771–1776. <https://doi.org/10.3892/ol.2013.1280>
38. Zhao K, Ma L, Feng L, Huang Z, Meng X, Yu J (2021) CD155 Overexpression Correlates With Poor Prognosis in Primary Small Cell Carcinoma of the Esophagus. *Front Mol Biosci*. <https://doi.org/10.3389/fmolb.2020.608404>
39. Wang R-B et al (2020) Overexpression of CD155 is associated with PD-1 and PD-L1 expression on immune cells, rather than tumor cells in the breast cancer microenvironment. *World J Clin Cases* 8(23):5935–5943. <https://doi.org/10.12998/wjcc.v8.i23.5935>
40. “The Cancer Genome Atlas Program - National Cancer Institute,” Jun. 13, 2018. <https://www.cancer.gov/about-nci/organization/ccg/research/structural-genomics/tcga>. Accessed 20 Feb 2021
41. Koch A, De Meyer T, Jeschke J, Van Criekinge W (2015) MEX-PRESS: visualizing expression, DNA methylation and clinical TCGA data. *BMC Genomics* 16:636. <https://doi.org/10.1186/s12864-015-1847-z>
42. O’Donnell JS, Long GV, Scolyer RA, Teng MWL, Smyth MJ (2017) Resistance to PD1/PDL1 checkpoint inhibition. *Cancer Treat Rev* 52:71–81. <https://doi.org/10.1016/j.ctrv.2016.11.007>
43. O’Donnell JS, Madore J, Li X-Y, Smyth MJ (2020) Tumor intrinsic and extrinsic immune functions of CD155. *Semin Cancer Biol* 65:189–196. <https://doi.org/10.1016/j.semcancer.2019.11.013>
44. Lupo KB, Matosevic S (2020) CD155 immunoregulation as a target for natural killer cell immunotherapy in glioblastoma. *J Hematol Oncol* 13(1):76. <https://doi.org/10.1186/s13045-020-00913-2>
45. Chauvin J-M et al (2015) TIGIT and PD-1 impair tumor antigen-specific CD8⁺ T cells in melanoma patients. *J Clin Invest* 125(5):2046–2058. <https://doi.org/10.1172/JCI80445>
46. Smazynski J et al (2020) The immune suppressive factors CD155 and PD-L1 show contrasting expression patterns and immune correlates in ovarian and other cancers. *Gynecol Oncol* 158(1):167–177. <https://doi.org/10.1016/j.ygyno.2020.04.689>
47. Huang D-W, Huang M, Lin X-S, Huang Q (2017) CD155 expression and its correlation with clinicopathologic characteristics, angiogenesis, and prognosis in human cholangiocarcinoma. *Oncotargets Ther* 10:3817–3825. <https://doi.org/10.2147/OTT.S141476>
48. Qu P et al (2015) Loss of CD155 expression predicts poor prognosis in hepatocellular carcinoma. *Histopathology* 66(5):706–714. <https://doi.org/10.1111/his.12584>

Publisher’s Note Springer Nature remains neutral with regard to jurisdictional claims in published maps and institutional affiliations.